Article

Multi-Objective Optimization of Thin-Film Silicon Solar Cells with Metallic and Dielectric Nanoparticles

Giovanni Aiello, Salvatore Alfonzetti *, Santi Agatino Rizzo and Nunzio Salerno

Department of Electrical, Electronic and Computer Engineering, University of Catania, Viale A. Doria 6, I-95125 Catania, Italy; giovanni.aiello@dieei.unict.it (G.A.); santi.rizzo@dieei.unict.it (S.A.R.); nunzio.salerno@dieei.unict.it (N.S.)

* Correspondence: alfo@dieei.unict.it; Tel.: +39-095-738-2320

Abstract: Thin-film solar cells enable a strong reduction of the amount of silicon needed to produce photovoltaic panels but their efficiency lowers. Placing metallic or dielectric nanoparticles over the silicon substrate increases the light trapping into the panel thanks to the plasmonic scattering from nanoparticles at the surface of the cell. The goal of this paper is to optimize the geometry of a thin-film solar cell with silver and silica nanoparticles in order to improve its efficiency, taking into account the amount of silver. An efficient evolutionary algorithm is applied to perform the optimization with a reduced computing time.

Keywords: renewable energy; solar cell; nanoplamonics; optimization; evolutionary algorithms; finite element method

1. Introduction

Concerns about environmental safety and energy resource provision are driving towards an increasing diffusion of technologies based on renewable energy [1]. Therefore, a great effort in designing advanced and inexpensive renewable energy generators has been emphasized for decarbonizing electricity supplies [2]. In this perspective, solar energy technologies are very promising and can replace fossil fuels thanks to some advantages: unlimited primary energy resource, easy installation, no pollution, and so on [3]. Silicon technology is the most used one for solar cells, mainly due to a good efficiency-to-cost ratio and great reliability [4].

The development of thin-film solar cells significantly reduces the amount of silicon needed to produce photovoltaic systems and the cost of the fabrication process, too [5]. On the other hand, as the thickness of the absorption (or the active) layer decreases, the energy-conversion efficiency drops dramatically and this is the main drawback of thin-film solar cells.

Recently, some researchers have shown that the scattering of solar radiation from nanoparticles, if suitably located and sized, may considerably improve the functioning of the thin-film cells [6–8]. The light is scattered and trapped into the silicon substrate by multiple and high-angle scattering, causing an increase of the effective optical path length in the cell and, consequently, enabling the improvement of its efficiency. Such a benefit is obtained thanks to the plasmon resonances [9], that is the intensification of the electromagnetic field around the nanoparticles placed over the top of the silicon substrate that look to be wider than their geometrical sizes [10,11]. Since the first work exploiting such an option [12], many papers have investigated thin-film solar cells enhanced by means of scattering from gold [13,14] and silver [15,16] nanoparticles. Similar improvements can also be obtained with dielectric nanoparticles [17,18]. In [19], it is shown that the placement of both metallic and dielectric nanoparticles is more advantageous than using only one type of nanoparticle. Moreover, some

structures with different nanoparticle radii and related distances between them are investigated to highlight their performances.

This paper aims to the optimization of a thin-film silicon solar cell by optimally sizing and positioning silver and silica nanoparticles on the top of the cell, in order to maximize the efficiency and minimize the amount of silver per square meter. The "parallel self-adaptive low-high evaluation evolutionary algorithm (PSALHE-EA)" [20,21] is applied to such optimization.

2. Finite Element Analysis of Light Scattering

The structure of the solar cell is shown in Figure 1, where the spherical nanoparticles are centered on the top of the silicon substrate at plane $z = 0$. For the sake of simplicity, the solar cell is considered infinitely extended in the x and y directions.
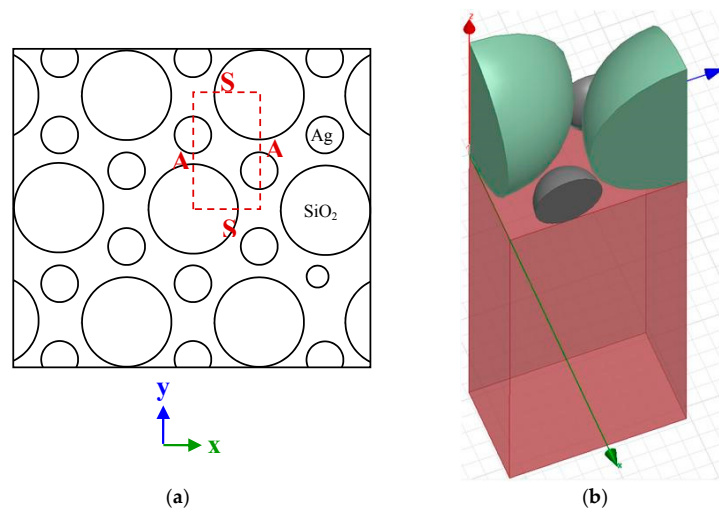
Figure 1. (**a**) Top view of the cell to be optimized. S stands for symmetric boundary condition and A for anti-symmetric. (**b**) 3D view of the analysis domain: the nanoparticles are placed at $z = 0$ and the domain is truncated at $z = 500$ nm and $z = -500$ nm by means of two perfectly matched layers.

A monochromatic electromagnetic wave at optical angular frequency ω, E-polarized along the x-axis, and travelling from the positive z-axis, radiates the cell:

$$\overline{E} = E_{max}e^{jk_0z}\,\hat{x} \tag{1}$$

The vector Helmholtz equation holds for this electromagnetic wave scattering problem:

$$\nabla \times \left(\mu_r^{-1}\nabla \times \overline{E}\right) - k_0^2\varepsilon_r\overline{E} = 0 \tag{2}$$

where μ_r and μ_0 are the relative and free-space magnetic permeability, respectively, ε_r and ε_0 are the relative and free-space electrical permittivity, respectively, and k_0 is the free-space wavenumber given by:

$$k_0 = \omega\sqrt{\varepsilon_0\mu_0} \tag{3}$$

At optical frequencies, the metallic nanoparticles give rise to plasmon resonances, which are taken into account by modeling them by means of a complex relative electric permittivity, experimentally determined [22]. Note that at these frequencies, the real part of the relative electric permittivity is negative.

For symmetry reasons, the analysis domain is restricted to the dashed rectangle in the xy plane shown in Figure 1, whereas in the z-direction the domain is truncated by means of two perfectly

matched layers (PMLs), placed at $z = 500$ nm and $z = -500$ nm. Since an objective of this work is to improve thin-film cell efficiency by increasing the optical transmission, the optimization is performed considering the silicon is thick enough to absorb all light transmitted into the silicon material as in [19]. The resulting domain is discretized by means of tetrahedral edge elements and the finite element analysis is performed by means of the ELFIN code [23,24] for various optical angular frequencies ω_m, $m = 1, \ldots, M$. The related fluxes W_m of the Poynting vector are computed as:

$$W_m = -\frac{1}{2} \iint_\Gamma Re\left\{\overline{E} \times \overline{H}^*\right\} \cdot \hat{z} \, dS \tag{4}$$

where the surface Γ is the $z = 0$ plane, $\hat{z}$ is the z-axis versor and H is the magnetic field. The domain is discretized by tetrahedral edge elements in such a way that the surface Γ is made of plane triangular patches. The generic k-th triangular patch T_k contributes to the integral in (4) with a value w_k given by:

$$w_k = \frac{1}{2\omega\mu_0} \sum_{i=1}^{N-1} \sum_{j=i+1}^{N} \left[Re\{E_i\}Im\{E_j\} - Re\{E_j\}Im\{E_i\} \right] q_{ij}^{(k)} \tag{5}$$

where N is the number of edges of the tetrahedron to which T_k belongs ($N = 6$ for first-order edge elements), indices i and j refer to two edges of the tetrahedron, E_i and E_j are the average values of the electric field along these edges, and q_{ij} are geometrical scalar values given by:

$$q_{ij}^{(k)} = \iint_{T_k} \left(\overline{\alpha}_i \times \nabla \times \overline{\alpha}_j - \overline{\alpha}_j \times \nabla \times \overline{\alpha}_i\right) \cdot \hat{n}_k \, dS \tag{6}$$

in which $\overline{\alpha}_i$ and $\overline{\alpha}_j$ are the vector shape functions of the i-th and j-th edges, respectively.

3. Multi-Objective Optimization Problem

The geometrical parameters to be optimized are the silica nanoparticle radius r, the ratio η between the silver and silica nanoparticle radii, and the distance d between them. The objective function $F_e(r,\eta,d)$ related to the efficiency to be maximized is obtained by computing the ratio between the number of photons absorbed per square meter per second and with respect to the incoming ones:

$$F_e(r, \eta, d) = \frac{\sum_{m=1}^{M} \frac{W_m}{W_{inc}} p_m}{\sum_{m=1}^{M} p_m} \tag{7}$$

in which W_m is the flux of the Poynting vector defined in (4); W_{inc} is the flux of the Poynting vector of the incident wave; and p_m is the number of incoming photons per square meter per second in the range $[\lambda_m - \Delta/2; \lambda_m + \Delta/2]$, where $\Delta = (\lambda_m - \lambda_{m-1})$.

Note that F_e is a pure number in the range [0, 1], whose computation requires a considerable computing time. Therefore, the evaluation of the objective function for all the combinations of geometrical parameter values (exhaustive analysis) is impracticable. Consequently, the optimization algorithm must solve the optimization problem by using few computations of the objective function.

The silver consumption objective function $F_{sc}(r,\eta,d)$ is obtained for a given geometry by the ratio between the volume C of silver per square meter and the maximum consumption C_{max}:

$$F_{sc}(r, \eta, d) = \frac{C}{C_{max}} \tag{8}$$

where $C_{max} = 4\sqrt{3}\pi r_{max}/27$ obtained when the maximum radius r_{max} of the silver nanoparticle and a distance d equal to 0 are considered. Also, this objective function is a pure number in the range [0, 1], but, on the contrary of F_e, it is to be minimized. Consequently, maximizing the function $1 - F_{sc}$ enables reduction of the consumption of silver per square meter.

A single objective function *F* can be obtained by weighting the two objective functions in order to simultaneously account for both targets:

$$F(r, \eta, d) = \rho F_e + (1 - \rho)(1 - F_{sc}) \tag{9}$$

where ρ is a weighting coefficient (0 < ρ < 1) whose value is chosen by the designer according to the relevance of each target. For example:

ρ = 1 implies that only the efficiency is optimized;
ρ = 0 implies that only the silver consumption is optimized (in this case, the solution is trivial);
ρ = 0.5 implies that the two targets have the same relevance.

Therefore, values of ρ greater than 0.5 mean that maximizing the efficiency is considered more relevant than the silver reduction. Finally, in order to optimize the solar cell the weighted objective function, *F* must be maximized.

Usually, an objective function weighting two conflicting objective functions is multimodal, i.e., there are several comparable good solutions. Moreover, in the specific optimization problem, an exhaustive search is impracticable due to the relevant time necessary to simulate numerically the 3D structure of Figure 1 in order to evaluate F_e. Consequently, it is very difficult to explore properly the multiple optima of the optimization problem by using a standard algorithm for global search, such as "simulated annealing (SA)" [25] or "genetic algorithm (GA)" [26]. Recently, the authors developed a coupled stochastic-deterministic algorithm [27] able to face this kind of optimization problem and an improved parallel version of the algorithm, PSALHE-EA [20], very useful when the objective function evaluation is time consuming.

The stochastic section of PSALHE-EA is a niche-based evolutionary algorithm [28]. Its main steps are shown in Figure 2. For a given individual (that is for a geometric configuration), two fitness values F_H and F_L are defined directly and inversely proportional to the objective *F*, respectively. The F_H value is penalized by a reduction factor if the individual falls inside a niche already associated with a maximum. Similarly, the F_L value is penalized by an increase factor if the individual falls inside a niche already associated to a minimum. Moreover, both values F_H and F_L are further penalized when the individual is located in a crowed zone. A roulette wheel with slots proportional to F_H is used to find the maxima of the multimodal function *F*, which are the optima of the optimization problem. Another roulette wheel with slots proportional to F_L is used to find the minima. Minima are used to find the niche radius related to each maximum. In fact, for a given maximum, the niche radius is the distance from the closest minimum.

A counter is associated with each individual, and when the individual, selected by means of the first roulette, generates a worse individual, the last one is rejected and the counter of the former is incremented by one. An individual of the current population is considered as a maximum when, for several consecutive times, it generates individuals with lower *F* (a threshold is considered for the counter), then it is stored in the "hypothetical" maxima database and replaced by a new individual randomly generated. On the other hand, it is replaced by the generated individual if it is better than the parent, and the counter of the new individual is set to the value of the parent reduced by one. Similar considerations hold for selection by means of the second roulette and new "hypothetical" minima. When at least one stop criterion is satisfied, the stochastic section stops. When a maximum A falls inside the niche of a maximum B, that is the distance between them is lower than the niche radius of B, and B falls inside the niche of A, the worst is considered as a "doublet" and it is removed from the database.

After this, the doublets are deleted, the remaining maxima are passed to the deterministic section—that is a patter search (PS) [29]—and its main steps are reported in Figure 3. The PS is applied to each maximum in the database and then the niche radius is updated using the minima. The algorithm could move more than one maximum towards the same hill and this means that new doublets are found and therefore removed.
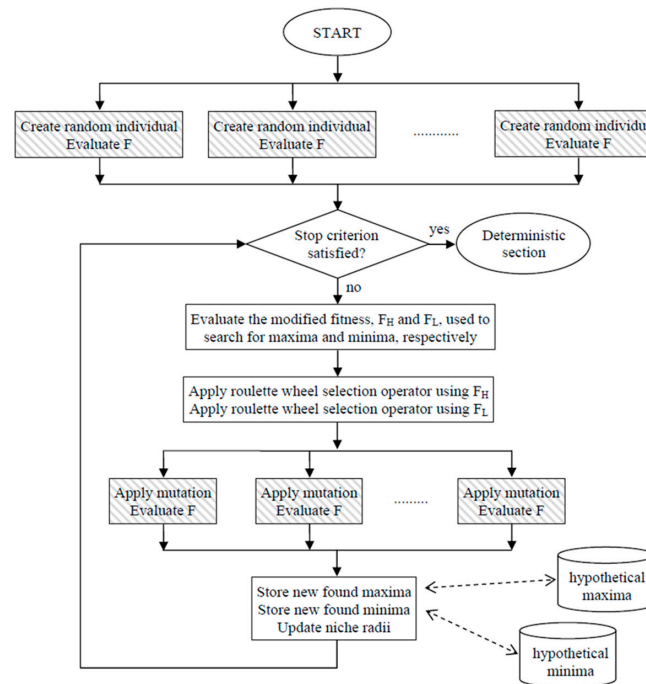
Figure 2. Main steps of the PSALHE-EA's stochastic section. In the blocks filled with grey lines the ELFIN program executes the finite element analysis in order to evaluate F_e used to obtain F. PSALHE-EA: parallel self-adaptive low-high evaluation-evolutionary algorithm.
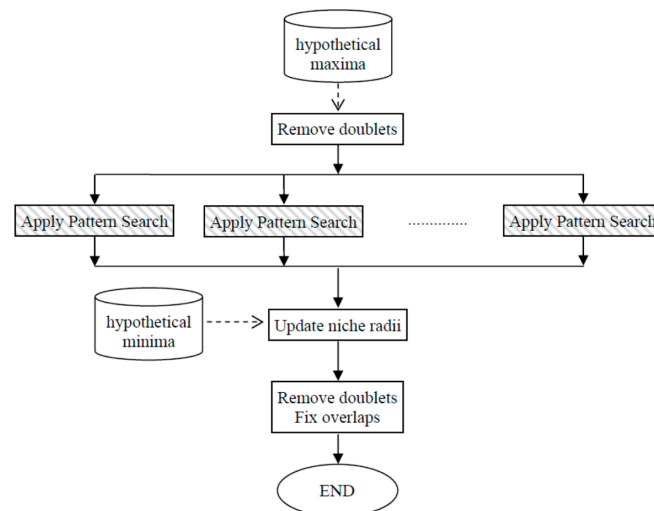
Figure 3. Main steps of the PSALHE-EA's deterministic section. In the blocks filled with grey lines, the ELFIN program executes the finite element analysis in order to evaluate F_e used to obtain F.

Finally, if the distance between two maxima is lower than the sum of their niche radii, the niche radii are reduced to make the niches tangent. The surviving maxima are the solutions that the algorithm supposes to be optima (global and local) of the multimodal function, and their niche radius can be considered as a measure of robustness with respect to the parameter variations.

4. Numerical Results

The ranges of the geometrical parameters to be optimized are reported in Table 1. A weighting coefficient ρ equal to 0.5 is considered for the objective function F in Equation (9). The efficiency objective function F_e in Equation (7) is computed for $M = 8$ different wavelengths in the range

[400, 1100] nm, with a step of 100 nm. The number of generations is set to 100 and the population size is set to 20. At each generation, four selections are carried out using a roulette with slots proportional to F_H and other four using a roulette with slots proportional to F_L. Then the objective functions F of the mutated individuals are computed simultaneously thanks to the parallelism of the algorithm. The thresholds related to the hypothetical maxima and minima are set to 10 and 7, respectively. In each generation, the crowding factor related to each individual in the population is computed by using the four individuals closest to it. Finally, each individual generating offspring with an objective function similar to its value for three consecutive times is considered to be placed in a flat area and it is substituted by a new randomly-generated individual.

Table 1. Ranges of the geometrical parameters to be optimized.

Parameter	Minimum	Maximum
r	20 nm	200 nm
η	0.05	1
d	0 nm	50 nm

The stochastic section performed a total number of 827 objective function evaluations, finding four hypothetical maxima. Since there was no doublet, the PS algorithm was applied starting from each of the four maxima. The starting step was set to 1/10 of the niche radius, the reduction degree of the step was set to a quarter of the last value and not more than three further reductions were considered to stop the PS. Since, for each optimization parameter, the PS explores two directions, by increasing and decreasing the parameter value, the minimum number of objective function evaluations performed by PS for each maximum is equal to 18. The PS performed a total of 177 objective functions evaluations. Note that one of the four hypothetical maxima found in the stochastic section, was considered by the algorithm as equivalent to another one and, as a consequence, it was eliminated. Table 2 reports the doublet and the hypothetical maximum held. The optimization was performed on a PC HP Pavillon h8-1551it, 2 Intel Core i7 2600 4 cores 3.4 GHz, 8 Gb RAM exploiting eight cores. The computing time reduced to less a quarter of that required for a serial execution.

The global optimum (max_1) and the two local maxima (max_2 and max_3) found by PSALHE-EA are reported in Table 2.

Table 2. Maxima found by means of PSALHE-EA.

Section	Parameter	max_1	max_2	max_3
	r	155.96	71.31	29.72
Stochastic	η	0.4393	0.0658	0.0663
	d	30.73	46.52	12.60
	F	0.8844	0.8810	0.8570
	PS evaluations	33	24	22
	r	129.75	89.59	30.04
	η	0.4163	0.0658	0.0663
	d	30.73	41.55	12.60
Deterministic	F	0.8947	0.8922	0.8584
	F_e	0.868	0.785	0.717
	F_{sc}	0.078	0.0003	0.0001
	niche radius	0.3299	0.4638	0.4844

The maxima are located in different regions of the optimization variable search space. The maximum max_1 enables to obtain an average efficiency (F_e) greater than the others but it requires a greater silver consumption. The silver consumptions related to max_2 and max_3 are very small. The former reaches such a desired result by considering small silver nanoparticles far among them, the latter by using smaller silver nanoparticles although their distance is reduced with respect to max_2. Finally, the niche radius of each solution is large enough to expect little performance degradation due to the fabrication process. Figure 4 shows the expected efficiency of the optimized cell at various

wavelengths for the global optimum. The efficiency is significantly improved at all wavelengths with respect to the solar cell without nanoparticles. Moreover, these results confirm that the use of both kinds of nanoparticles enable us to reach better performances with respect to the cases where only one kind of nanoparticle is considered.

The number of photons per second per square meter has been computed by means of AM 1.5 (global-tilt) solar spectrum [30], obtaining 2.40×10^{21}, 2.17×10^{21} and 1.98×10^{21} respectively for max_1, max_2 and max_3. The number of photons per second per square meter related to max_1 is similar to the optimum (2.38×10^{21}) reported in [19], that was obtained for $r = 100$ nm, $\eta = 0.5$ and $d = 8$ nm. The related F_{sc} is equal to 0.111, consequently, the optimum in [19] requires much more silver compared to the maximum found in this paper (+42%).
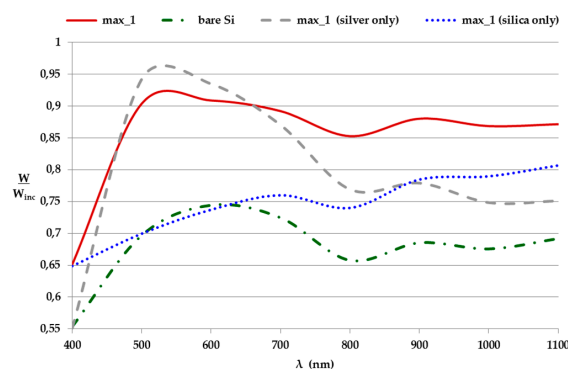

Figure 4. Efficiency of the optimized cell (max_1).

Figure 5 shows the magnitude of the modulus of the electrical field E at the silicon surface (plane $z = 0$) for the nanoparticle layout of max_1 at $\lambda = 500$ nm. The intensification of the electromagnetic field around the silver nanoparticles shown in Figure 5 highlights that they look to be wider than their geometrical sizes thanks to the plasmon resonance and, consequently, the light is scattered and trapped into the silicon substrate, improving the solar cell efficiency [10,11].
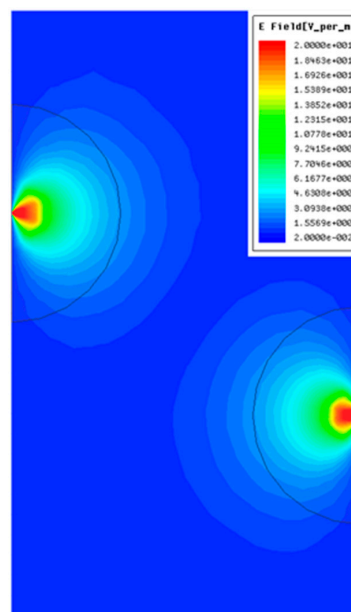

Figure 5. Magnitude of the electrical field, *E*, at plane *z* = 0 of the analysis domain when max_1 and $\lambda = 500$ nm are considered. The two semicircles represent the top view of the silver nanoparticles in the analysis domain.

To test the goodness of the optimal geometrical configuration found considering a real thin-film layer of silica instead of an infinite one, a simulation has been performed for the max_1 configuration considering a silica thickness of 1 μm. The calculated number of photons per second per square meter was 0.859×10^{21}, which is about one-third of the value obtained considering an infinite silica layer.

Then, a further optimization has been performed considering a solar cell of 1 μm thickness in order to search for solutions with better efficiency, taking into account the silver consumption, too. Also in this case the optimization algorithm found three maxima, which are reported in Table 3. The number of photons per second per square meter is equal to 1.07×10^{21}, 1.16×10^{21}, and 1.21×10^{21} respectively for max_a, max_b, and max_c. An increment of about 40% is obtained with respect to the thin-film solar cell with nanoparticles placed atop of it as in max_1 and, furthermore, with a reduced silver quantity.

Table 3. Maxima found by means of PSALHE-EA considering a 1 μm-thin-film solar cell.

Parameter	max_a	max_b	max_c
r	65.5	155	144
η	0.199	0.349	0.485
d	37	2.63	33.9
F	0.693	0.666	0.658
F_e	0.389	0.422	0.438
F_{sc}	0.004	0.081	0.122
niche radius	0.463	0.644	0.32

Finally, the efficiency of a solar cell with infinite thickness has been computed considering the nanoparticles configuration related to max_a, obtaining 2.04×10^{21} photons per second per square meter. Thus, the comparison of the maxima found in the two cases confirms that the optimal solution for a solar cell with very large thickness is not the best one for a thin-film solar cell and vice versa. Nevertheless, PSALHE-EA was able to optimize the solar cell with very large thickness obtaining an efficiency value similar to that reported in [19] with the advantage of a strong reduction of silver and to also optimize the thin-film solar cell obtaining an acceptable number of photons with small silver consumption.

5. Conclusions

In this paper, the optimization of a thin-film silicon solar cell has been performed by optimally sizing and positioning silver and silica nanoparticles on the top of the cell. The optimization aims at maximizing the cell efficiency and minimizing the silver amount.

The optimization has been carried out by means of PSALHE-EA, a parallel self-adaptive low-high-evaluation evolutionary algorithm, developed by the authors for multimodal optimizations. In the optimizations performed, the algorithm has found three optima with an acceptable number of FEM simulations. Moreover, the parallelism of the PSALHE-EA notably reduces the overall computing time.

If an infinite thickness is considered, the optimum found by PSALHE-EA enables an efficiency similar to that reported in [19] with the advantage of a strong reduction of silver. The optimization has been performed also considering a thin-film solar cell with a thickness equal to 1 μm. The comparison of the maxima found in the two cases has confirmed that the optimal solution for a solar cell with very large thickness is not the best one for a thin-film solar cell and vice versa. Nevertheless, PSALHE-EA was able to optimize both solar cells obtaining good efficiency with small silver consumption.

Author Contributions: All authors contributed equally to this work.

References

1. Bauen, A. Future energy sources and systems—Acting on climate change and energy security. *J. Power Sources* **2006**, *157*, 893–901. [CrossRef]

2. Mercure, J.-F.; Pollitt, H.; Chewpreecha, U.; Salas, P.; Foley, A.M.; Holden, P.B.; Edwards, N.R. The dynamics of technology diffusion and the impacts of climate policy instruments in the decarbonisation of the global electricity sector. *Energy Policy* **2014**, *73*, 686–700. [CrossRef]

3. Graditi, G.; Ferlito, S.; Adinolfi, G.; Tina, G.M.; Ventura, C. Performance estimation of a thin-film photovoltaic plant based on an artificial neural network model. In Proceedings of the 2014 5th International Renewable Energy Congress (IREC), Hammamet, Tunisia, 25–27 March 2014.

4. Singh, R. Why silicon is and will remain the dominant photovoltaic material. *J. Nanophotonics* **2009**, *3*. [CrossRef]

5. Green, M.A.; Zhao, J.; Wang, A.; Wenham, S.R. Very high efficiency silicon solar cells-science and technology. *IEEE Trans. Electron. Devices* **1999**, *46*, 1940–1947. [CrossRef]

6. Pillai, S.; Catchpole, K.R.; Trupke, T.; Green, M.A. Surface plasmon enhanced silicon solar cells. *J. Appl. Phys.* **2007**, *101*, 093105. [CrossRef]

7. Hägglund, C.; Zäch, M.; Petersson, G.; Kasemo, B. Electromagnetic coupling of light into a silicon solar cell by nanodisk plasmons. *Appl. Phys. Lett.* **2008**, *92*. [CrossRef]

8. Lee, H.-C.; Wu, S.-C.; Yang, T.-C.; Yen, T.-J. Efficiently harvesting sun light for silicon solar cells through advanced optical couplers and a radial p-n junction structure. *Energies* **2010**, *3*, 784–802. [CrossRef]

9. Kreibig, U.; Vollmer, M. *Optical Properties of Metal Clusters*; Springer Series in Materials Science; Springer: New York, NY, USA, 1995; Volume 25.

10. Pillai, S.; Green, M.A. Plasmonics for photovoltaic applications. *Sol. Energy Mater. Sol. Cells* **2010**, *94*, 1481–1486. [CrossRef]

11. Atwater, H.A.; Polman, A. Plasmonics for improved photovoltaic devices. *Nat. Mater.* **2010**, *9*, 205–213. [CrossRef] [PubMed]

12. Stuart, H.R.; Hall, D.G. Island size effects in nanoparticle-enhanced photodetectors. *Appl. Phys. Lett.* **1998**, *73*, 3815–3817. [CrossRef]

13. Schaadt, D.M.; Feng, B.; Yu, E.T. Enhanced semiconductor optical absorption via surface Plasmon excitation in metal nanoparticles. *Appl. Phys. Lett.* **2005**, *86*, 063106:1–063106:3. [CrossRef]

14. Qu, D.; Liu, F.; Yu, J.; Xie, W.; Xu, Q.; Li, X.; Huang, Y. Plasmonic core-shell gold nanoparticle enhanced optical absorption in photovoltaic devices. *Appl. Phys. Lett.* **2011**, *98*. [CrossRef]

15. Wang, E.C.; Mokkapati, S.; Soderstrom, T.; Varlamov, S.; Catchpole, K.R. Effect of nanoparticle size distribution on the performance of plasmonic thin-film solar cells: Monodisperse versus multidisperse arrays. *IEEE J. Photovolt.* **2013**, *3*, 267–270. [CrossRef]

16. Temple, T.L.; Mahanama, G.D.K.; Reehal, H.S.; Bagnall, D.M. Influence of localized surface plasmon excitation in silver nanoparticles on the performance of silicon solar cells. *Sol. Energy Mater. Sol. Cells* **2009**, *93*, 1978–1985. [CrossRef]

17. Chen, C.P.; Lin, P.H.; Chen, L.Y.; Ke, M.Y.; Cheng, Y.W.; Huang, J.J. Nanoparticle-coated n-ZnO/p-Si photodiodes with improved photoresponsivities and acceptance angles for potential solar cell applications. *Nanotechnology* **2009**, *20*. [CrossRef] [PubMed]

18. Akimov, Y.A.; Koh, W.S.; Sian, S.Y.; Ren, S. Nanoparticle-enhanced thin-film solar cells: Metallic or dielectric nanoparticles. *Appl. Phys. Lett.* **2010**, *96*. [CrossRef]

19. Yeh, Y.M.; Wang, Y.S.; Li, J.H. Enhancement of the optical transmission by mixing the metallic and dielectric nanoparticles atop the silicon substrate. *Opt. Express* **2011**, *19*, A80–A94. [CrossRef] [PubMed]

20. Dilettoso, E.; Rizzo, S.A.; Salerno, N. A parallel version of the self-adaptive low-high evaluation evolutionary-algorithm for electromagnetic device optimization. *IEEE Trans. Magn.* **2014**, *50*, 633–636. [CrossRef]

21. PSALHE: An Algorithm to Solve Multimodal Optimization Problems. Available online: http://wwwelfin.diees.unict.it/esg/ricerca/psalhe/index.phtml (accessed on 21 July 2016).

22. Johnson, P.B.; Cristy, R.W. Optical constants of the noble metals. *Phys. Rev. B* **1972**, *6*, 4370–4379. [CrossRef]

23. Aiello, G.; Alfonzetti, S.; Borzì, G.; Salerno, N. An overview of the ELFIN code for finite element research in electrical engineering. In *Software for Electrical Engineering Analysis and Design*; Konrad, A., Brebbia, C.A., Eds.; WIT Press: Southampton, UK, 1999.
24. Aiello, G.; Alfonzetti, S.; Brancaforte, V.; Chiarello, V.; Salerno, N. Applying FEM-RBCI to the analysis of plasmons in metallic nanoparticles. *Int. J. Appl. Electromagn. Mech.* **2012**, *39*, 13–20.
25. Alfonzetti, S.; Dilettoso, E.; Salerno, N. Simulated annealing with restarts for the optimization of electromagnetic devices. *IEEE Trans. Magn.* **2006**, *42*, 1115–1118. [CrossRef]
26. Alfonzetti, S.; Dilettoso, E.; Salerno, N. A proposal for a universal parameter configuration for genetic algorithm optimization of electromagnetic devices. *IEEE Trans. Magn.* **2001**, *37*, 3208–3211. [CrossRef]
27. Dilettoso, E.; Rizzo, S.A.; Salerno, N. SALHE-EA: A new evolutionary algorithm for multi-objective optimization of electromagnetic devices. In *Intelligent Computer Techniques in Applied Electromagnetics*; Wiak, S., Krawczyk, A., Dolezel, I., Eds.; Springer: Berlin, Germany, 2008.
28. Shir, O.M. Niching in evolutionary algorithms. In *Handbook of Natural Computing: Theory, Experiments, and Applications*; Springer: Berlin/Heidelberg, Germany, 2012; pp. 1035–1069.
29. Hooke, R.; Jeeves, T.A. "Direct search" solution of numerical and statistical problems. *J. Assoc. Comput. Mach.* **1961**, *8*, 212–229. [CrossRef]
30. Reference Solar Spectral Irradiance: Air Mass 1.5. Available online: http://rredc.nrel.gov/solar/spectra/am1.5/ (accessed on 21 July 2016).